Available online at www.sciencedirect.com
ScienceDirect
Radiation Measurements 43 (2008) 1417–1422
Radiation Measurements
www.elsevier.com/locate/radmeas

Analyses of light scattered from etched alpha-particle tracks in PADC

D. Nikezic, K.N. Yu*

Department of Physics and Materials Science, City University of Hong Kong, Tat Chee Avenue, Kowloon Tong, Kowloon, Hong Kong

Received 28 August 2007; received in revised form 16 November 2007; accepted 4 February 2008

Abstract

A computational model for light propagation through an etched alpha-particle track was described. Four different cases for light ray propagation through the etched track were studied in detail. The track profile, optical appearance and distribution of scattered light were given for three typical types of etched tracks. These laid the foundation for future automatic determination of properties of the alpha particles producing the tracks through the scattered light.

PACS: 07.05; 23.60; 29.40

Keywords: PADC; Tracks; Etching; Light; Simulation

1. Introduction

Solid-state nuclear track detectors (SSNTDs) are commonly used for radon measurements. One of the most widely used SSNTDs is made of polyallyldiglycol carbonate (PADC), which is commercially available as CR-39 detectors. A recent review on SSNTDs can be found in Nikezic and Yu (2004). For radon measurements and many other applications, etched tracks were studied using optical microscopes (see e.g., Yu et al., 2005). However, as expected, the procedures involved were tedious and time consuming. Automatic and semi-automatic systems are desirable, but the optical appearance of tracks or the scattered light intensity was involved.

There were only a few references in the literature on scattering of light from etched tracks in SSNTDs. In most of the cases, scattered light was used to measure track densities from experiments related to neutron dosimetry (Harvey and Weeks, 1987; Popov and Pressyanov, 1997; Meyer et al., 1997; Groetz et al., 1999). Groetz et al. (1998) developed a model for laser light scattering by nuclear tracks in CR-39 detectors. The model was based on wave optics and the so-called "*bi-directional scatter distribution function*" to describe scattered light patterns in two orthogonal planes.

Recently, studies of optical characteristics of etched tracks in PADC films using the *ray tracing method* were performed (Nikezic et al., 2005; Yu et al., 2007). Based on geometrical optics, a computer program called TRACK_VISION 1.0 (Nikezic and Yu, 2008; also available from http://www.cityu.edu.hk/ap/nru/vision.htm) was developed in our laboratory to simulate light propagation through the tracks and to calculate the brightness of all grid elements in the track wall. In the current paper, the model and the corresponding computer program were further developed to facilitate determination of the scattered pattern of light on a single track.

2. Model

As the first step, it is necessary to compute the points that belong to the track wall in three dimensions (3-D). First, the points on the track wall in two dimensions (or referred to as the track profile) were evaluated using our computer code TRACK_VISION 1.0. The 3-D track wall was then generated by rotating the curve representing the track profile around the particle trajectory. This was possible because of the isotropic nature of chemical etching of the track with respect to the particle trajectory. Planes parallel to the detector surface were then constructed to intersect with the 3-D track body. The intersections between these horizontal planes and the 3-D track were in general semi-elliptical curves or some more complicated closed

* Corresponding author. Tel.: +852 27 887 812; fax: +852 27 887 830.
E-mail address: peter.yu@cityu.edu.hk (K.N. Yu).

1350-4487/$ - see front matter © 2008 Elsevier Ltd. All rights reserved.
doi:10.1016/j.radmeas.2008.02.003

curves. The intersections could also be simply regular circles if the incidence of the alpha particle had been normal with respect to the detector surface.

During the computations, the coordinates of points representing these curves were stored in the computer memory. The number of points representing the horizontal curves was kept constant. A mesh of four-angle polygons was formed from these points to represent the track wall. Two vertices of these four-angle polygons belonged to one intersecting plane and the other two vertices to another plane. The procedures of forming polygons were applied for the entire track. In our calculations, all polygons were assumed flat. In fact, this was not true in general, particularly when the size of a polygon was relatively large and there was significant curvature for the corresponding portion of the track. For a proper representation of the track body, the polygons should be very small, so the number of intersecting planes and the number of points per one intersection plane should be sufficiently large. All the polygons were indexed with the corresponding numbers and their coordinates were stored in an array in the computer memory.

For the simulation of light propagation through the track, a line perpendicular to each surface was needed. While it was straightforward to determine the plane from three non-collinear points, we now had four points for each polygon surface, namely, T_1, T_2, T_3 and T_4, which were in general not coplanar. In the present approach, two normal lines were determined, the first one deriving from the points T_1, T_2 and T_3 while the second one from the points T_1, T_2 and T_4. The average normal, $\vec{N}(n_x, n_y, n_z)$, was then chosen to represent the corresponding polygon element.

Simulation of light passage through the track was based on geometrical optics in the present work. In practice, an etched alpha-particle track reached a size as large as 5–20 μm, which was about an order of magnitude larger than the wavelength of visible light (~ 0.5 μm), so that geometrical optics was applicable. Etched tracks smaller than 1 μm are usually not visible under the optical microscope and are irrelevant to practical applications.

The transmission mode of operation was considered for the optical microscope. Here, the light came from the bottom of the detector and entered the track body (assumed to be filled with air) from the detector material which was optically denser than air. The first task here was to determine which polygon was hit by the light ray. The ray was directed vertically upwards, i.e., perpendicular to the detector surface, and was characterized by the coordinates (x_0, y_0). The vector $\vec{p}(p_x, p_y, p_z) = \vec{p}(0, 0, 1)$ described the initial light direction. The coordinates (x_0, y_0) were compared with coordinates of all polygons to determine which polygon was actually hit. The problem was tackled through simple geometrical considerations. If the point was out of the polygon, the sum of angles subtended to all polygon lines should be smaller than 360°. On the contrary, if the point (x_0, y_0) was inside the polygon, the sum of angles should be equal to 360°. The angle α between the incident ray and the normal onto the corresponding polygon was determined through the equation

$$\alpha = \cos^{-1}(\vec{p} \cdot \vec{N}). \tag{1}$$

The next step was the determination of the refraction angle β based on Snell's refraction law as

$$n \sin\alpha = \sin\beta, \tag{2}$$

where n was the refraction index of the detector material (which was taken as 1.5 for PADC). The new direction of the ray was characterized by the vector $\vec{p}_1 = (p_{1x}, p_{1y}, p_{1z})$ which was obtained from the following set of equations:

$$\vec{p}_1 \cdot \vec{N} = \cos\beta, \tag{3}$$

$$\vec{p}_1 \cdot \vec{p} = \cos(\beta - \alpha), \tag{4}$$

$$\vec{p}_1 \cdot (\vec{p} \times \vec{N}) = 0. \tag{5}$$

Eq. (3) defined the angle between the new direction and the normal as β while Eq. (4) defined the angle between the new and old directions as (β–α). Eq. (5) imposed the condition that all three vectors $\vec{p}_1$, $\vec{p}$ and $\vec{N}$ were coplanar. A similar set of equations was applied to all refractions that occurred in this problem.

In some cases, total internal reflection occurred on the polygons. Here, somewhat different equations were required to find the new direction $\vec{p}_R$ of the reflected ray. If $\vec{p}$ was the initial direction of a light ray, and $\vec{N}$ was the normal to the polygon, the direction of the ray reflected from that polygon could be found from

$$\vec{p}_R \cdot \vec{N} = \cos\alpha, \tag{6}$$

$$\vec{p}_R \cdot \vec{p} = \cos(\pi - 2\alpha), \tag{7}$$

$$\vec{p}_R \cdot (\vec{p} \times \vec{N}) = 0. \tag{8}$$

For the computer simulations, the points from which the light rays came were sampled randomly using the Monte Carlo methodology.

2.1. Analyses of possible cases

Four different cases were possible when a light ray passed through an etched alpha-particle track. Three of them are schematically shown in Fig. 1.

Case 1: The light ray 1 was totally reflected from the track wall, and returned back into the detector material. It then came to the detector surface where it again underwent total internal reflection. The ray finally returned back into detector and did not contribute to the scoring of light scattered out of the detector (i.e., it was finally directed downwards in Fig. 1).

Case 2: The light ray 2 was refracted at the track interface. Here, the normal $\vec{N}$, incident angle α and the refracted angle β are shown. The ray exited from the track through the track opening.

Case 3: The light ray 3 was totally reflected from the track wall, and exited from the detector surface because the incidence angle there was smaller than the critical angle.

Case 4: This case is not shown in Fig. 1. The ray was refracted on the track interface, but then returned into the detector body due to geometrical considerations. This was possible when the alpha particle made an oblique incidence with the detector surface and when the track was well under the detector surface.

2.2. Scattered light intensity

To calculate the intensity of the light ray scattered from the etched alpha-particle track, a "detection hemisphere" with a radius R, which was much larger than the track dimensions, was constructed with the center at the point where the particle trajectory intersected with the post-etched detector surface. The hemisphere was divided into surface elements with steps of $\Delta\varphi = 1^\circ$ and $\Delta\theta = 1^\circ$, so a total of 32 400 elements were used. The surface areas of the elements were given by $\Delta S \approx R^2 \sin\theta\Delta\theta\Delta\varphi$, and each surface element was characterized by two angles, or with two index variables in the computer program. Although the calculations were performed for whole hemisphere, the distributions are given only in terms of the two angles, θ and φ.

2.3. Coordinate system

The coordinate system was chosen in the following way. The origin was at the point where the particle trajectory intersected with the post-etched detector surface. The z-axis was perpendicular to the detector surface and was directed out of the detector body. The x-axis was along the detector surface and represented the projection of the particle trajectory onto the detector surface. The y-axis was also along the detector surface and was orthogonal to the x- and z-axes. In such a geometry, the tracks were always symmetrical with respect to the plane $y = 0$.

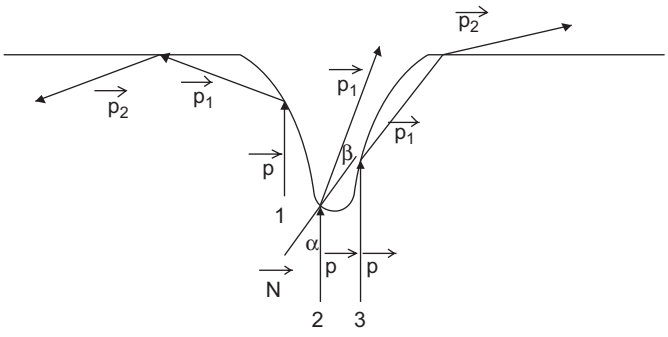

Fig. 1. Three possible ray paths in an alpha-particle track. The incident ray is represented by the vectors $\vec{p}$, the ray after the first reflection or first refraction is represented by $\vec{p}_1$ and that after the second reflection/refraction, if any, with $\vec{p}_2$. The normal $\vec{N}$ and angles α and β are shown only for the case 2.

3. Results

Results for selected characteristic cases are outlined in the following.

3.1. Vertical incidence, etched track in conical phase and steep track walls

Such an etched track could be obtained from a normally incident alpha particle with an incident energy of 5 MeV for an etching time 6 h (using the bulk etch rate $V_b = 1.3\,\mu m/h$). The number of intersecting planes was chosen as 500 and the number of points per one intersection plane was also chosen as 500. The number of simulation histories was 10^5. The profile of this track as well as the simulated optical appearance of this track when viewed from above, both determined using TRACK_VISION 1.0 are given in Fig. 2.

One can see that the track profile was almost triangular. In this energy range, the stopping power was not a strong function of the energy, and the track-etch rate V_t was almost constant. The track diameter was 9.15 μm and the track depth was 9.77 μm. At all points on the track wall, the light rays suffered from total internal reflection so that the track appearance was completely dark. In addition, all light rays would again undergo total internal reflection on the detector surface, so that no light scattered from this track could reach the detection hemisphere. The computer program developed for calculating the scattered light also detected no light from the detector. This could also be shown intuitively from simple geometrical considerations as shown in Fig. 3. If we neglected the curvature of the track profile, the half-cone angle was given by $\gamma = \tan^{-1}((D/2)/(\text{track depth}))$. The program gave the major axis as $D = 9.15\,\mu m$ and the track depth as 9.77 μm, so $\gamma = 25.1^\circ$. The incident angle on the detector surface was then $2\gamma = 50.2^\circ$, which was larger than the critical angle for total internal reflection given by $\theta_c = \sin^{-1}(1/n) = 41.8^\circ$.

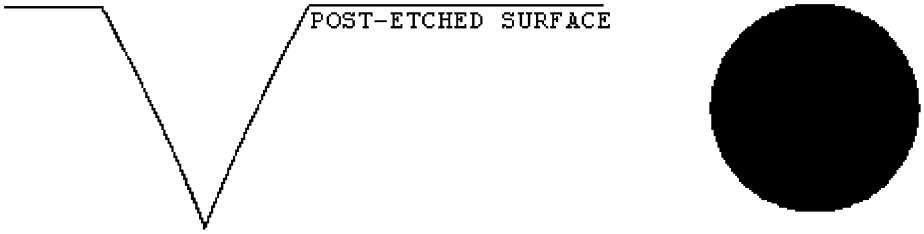

Fig. 2. An etched track from a normally incident 5-MeV alpha particle for an etching time of 6 h. The track profile (left) and the simulated optical appearance of this track when viewed from above (right).

3.2. Vertical incidence, etched track in spherical phase

Such an etched track could be obtained from a normally incident alpha particle with an incident energy of 2.5 MeV for an etching time 10 h. Other parameters for calculations were the same as those described in Section 3.1. The profile of this track as well as the simulated optical appearance of this track when viewed from above, both determined using TRACK_VISION 1.0 are given in Fig. 4.

The track was spherical in shape with a depth of 7.45 μm and the track-opening diameter was 18.9 μm. The light rays coming from below the track were refracted through very small angles in the central area. The intensity loss was therefore relatively small and the central part of the track was very bright. When going away from the central portion, the refracted angle increased and the intensity loss became slightly larger, so that the gray level was changed continuously and slightly (which might not be observed on computer screens with a low resolution). Finally, when the periphery of the track opening was approached, the track wall was sufficiently steep and total internal reflection occurred, resulting in a dark ring as observed on the right panel in Fig. 4.

The angular distribution of light scattered from this track is shown in Fig. 5. The distribution of θ showed one pronounced maximum at 0°, which decreased gradually up to about 40°. This part of the distribution originated from the light that passed through the track without total internal reflection and refracted under relatively small angles. For the light rays totally reflected from the track, some would return to the detector body due to total internal reflection from the detector surface, while some would exit from the detector and be scattered under large angles. The latter part (i.e., the part exiting from the detector) was seen in the distribution curve in the range from 65° to 90°.

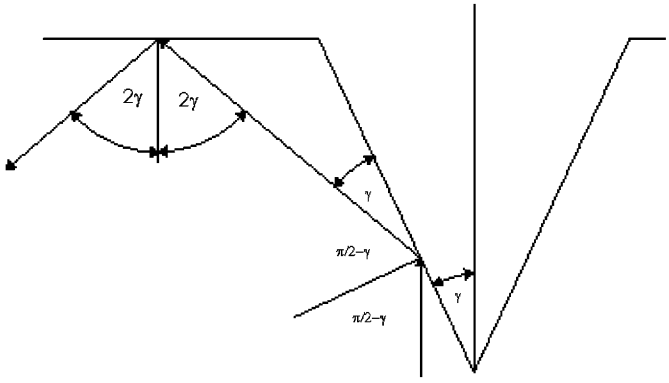

Fig. 3. A simplified geometrical consideration showing that no light is coming out from the track presented in Fig. 2.

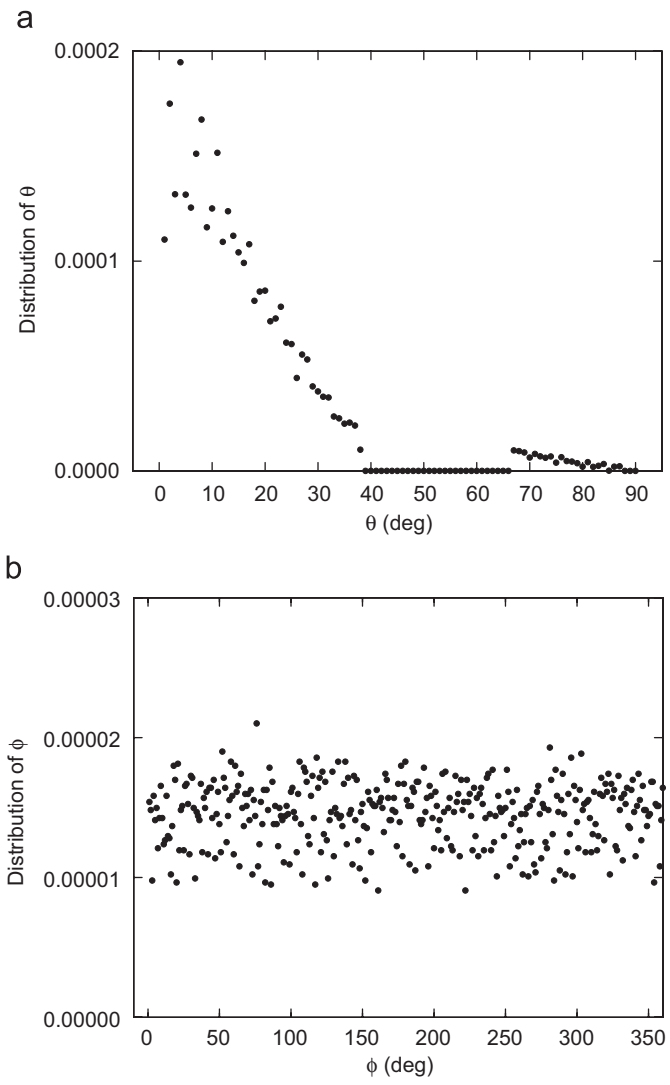

Fig. 5. Distribution of angle θ (panel (a)) and angle φ (panel (b)) for the track presented in Fig. 4.

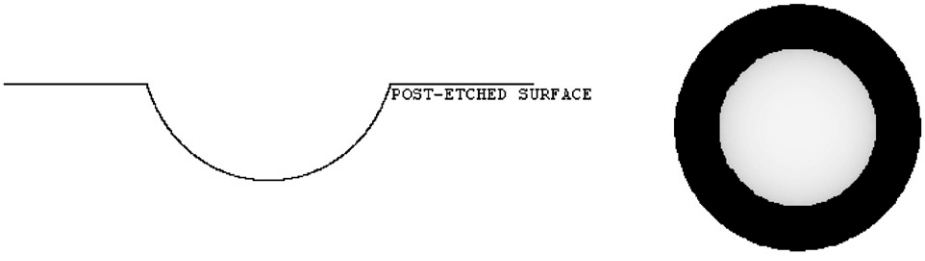

Fig. 4. An etched track from a normally incident 2.5-MeV alpha particle for an etching time of 10 h. The track profile (left) and the simulated optical appearance of this track when viewed from above (right).

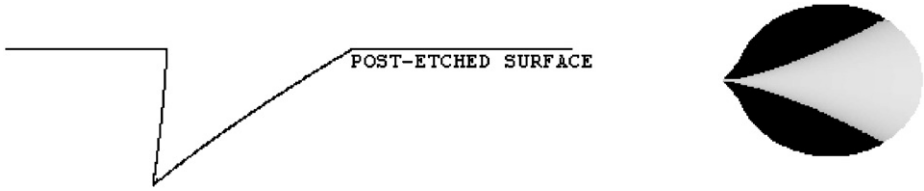

Fig. 6. An etched track from a 5-MeV alpha particle with an incidence angle of 60° for an etching time of 6 h. The track profile (left) and the simulated optical appearance of this track when viewed from above (right).

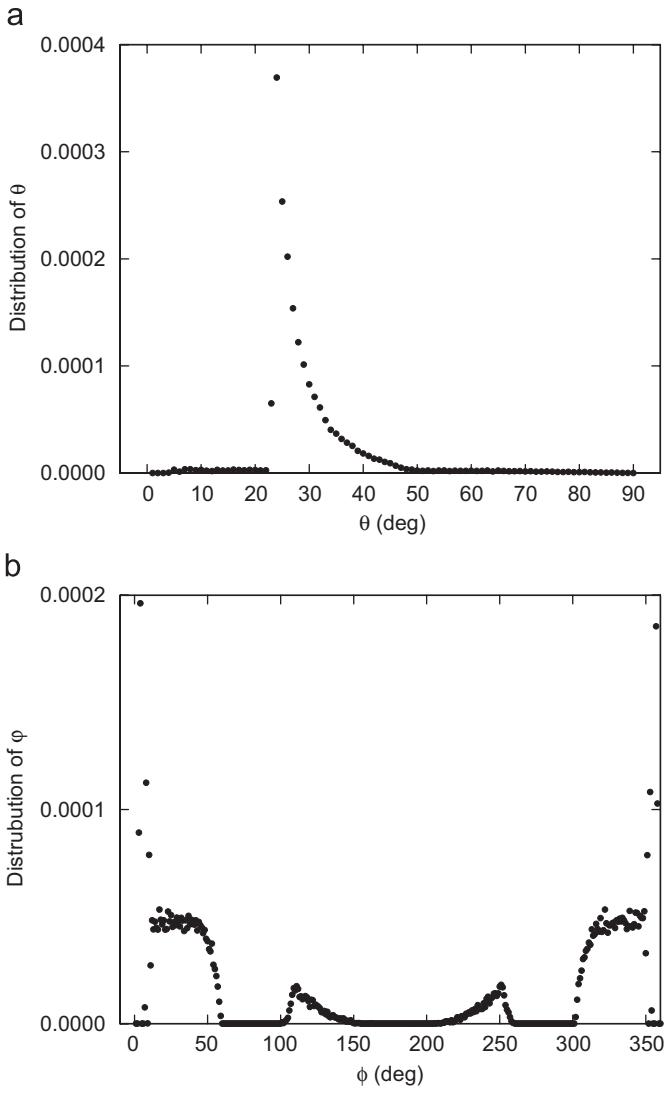

Fig. 7. Distribution of angle θ (panel (a)) and angle φ (panel (b)) for the track presented in Fig. 6.

This track was symmetrical with respect to the z-axis, so a uniform distribution of scattered light with respect to the angle φ was expected. This was indeed obtained as shown in Fig. 5(b). Some scattering of data was present, which was due to the poor statistics. Since the angle φ had a range from 0° to 360° and the step was 1°, an average of only 277 hits in each angle interval was expected. A larger number of simulations would give better statistics but at the same time would need too long computational time.

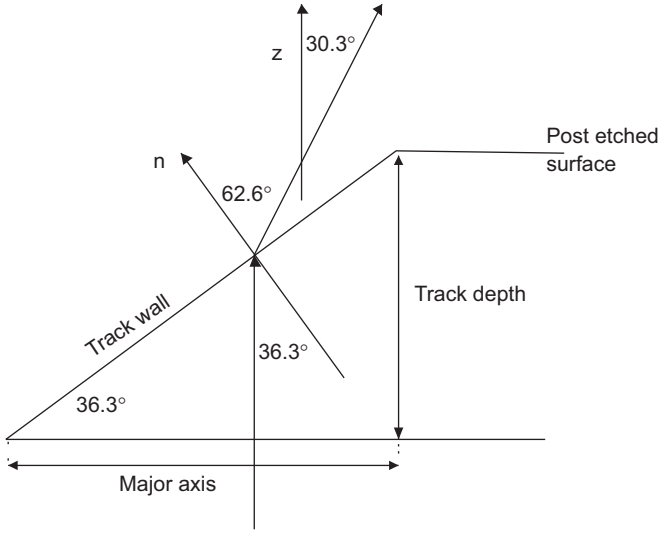

Fig. 8. Analysis of angles for the track shown in Fig. 6. The light ray is deflected by an angle $\theta = 30.3°$ with respect to the z-axis, which is perpendicular to the detector surface.

3.3. Oblique incidence, etched track in conical phase

Such an etched track could be obtained from an alpha particle with an incident energy of 5 MeV and incident angle of 60°. Etching was performed for 6 h. Other parameters for calculations were the same as those described in Section 3.1. The profile of this track as well as the simulated optical appearance of this track when viewed from above, both determined using TRACK_VISION 1.0 are given in Fig. 6.

The track depth was 7.4 μm and the major and minor axes were 10.1 and 8.26 μm, respectively. This track was in the conical phase. A part of the track wall (the left portion of the track shown in Fig. 6) was almost vertical and this was in fact extended to the right portion in the 3-D space. These steep walls led to total internal reflection of light, which was revealed as the dark part of the track when viewed from the above. The other part of the track wall (the right portion of the track shown in Fig. 6) had such an inclination angle so that light could pass with some refraction and this portion was revealed as the bright part of the track when viewed from the above. The angular distributions of the scattered light are shown in Figs. 7(a) and (b).

In Fig. 7(a), the distribution of scattered light with the angle θ is shown. Here, a very strong peak exists at about 30°. A simplified analysis of angles is shown in Fig. 8. Since the

track depth was 7.41 μm and the major axis was 10.1 μm, the inclination angle of the track wall along the major axis was $\alpha = \tan^{-1}$ (track depth/(D)) = 36.3°.

When going away from the major axis of the track opening, the angle between the light ray and the normal to the track wall increased and the angle between the scattered light ray and the z-axis also increased. Finally we came to a point where the angle became larger than the critical angle θ_c and total internal reflection occurred. This qualitatively explained the results shown in Fig. 7(a). However, the explanation for the distribution of the angle φ is much more complicated. We will not go into the details here but would like to remark that the distribution was again symmetric, which could be explained by the symmetry of the track with respect to the plane $y = 0$ (plane to which the major axis belonged and from which the angle φ was measured).

4. Conclusion

The present model and the corresponding computer programs enabled determination of the track profile, opening contour (not shown here), optical appearance and finally the distribution of the scattered light. In real experiments, it will be difficult, if not impossible, to measure the intensity of light scattered from one single track. However, consideration of the scattering from a single track is a starting point. The next step will be extension to a set of tracks which are obtained under the same irradiation and etching conditions. Such tracks should be identical to one another and summing of scattered intensities from one track should be performed. Another extension will be consideration of a set of different tracks obtained from various incident energies and angles and with various orientations (as in the case of radon measurements). In this case, scattering will be calculated from all individual tracks and summed up.

The examples in the present paper showed that distribution of scattered light depended on the track characteristics and track orientation. These results demonstrated the feasibility of methods studying track characteristics using the scattered light. Systematical comparisons between experimental and theoretical results will be made in a forthcoming paper, which will be needed before such methods can be put into practice.

Acknowledgment

The present work was supported by a research Grant CityU123106 from the Research Grants Council of the HKSAR.

References

Groetz, J.E., Lacourt, A., Chambaudet, A., 1998. Coherent light scattering by nuclear etched tracks in PADC (a form of CR-39). Nucl. Instrum. Meth. B. 142, 503–514.

Groetz, J.E., Lacourt, A., Meyer, P., Fromm, M., Chambaudet, A., Potter, J., 1999. A new method for reading CR-39 by using coherent light scattering. Radiat. Prot. Dosim. 85, 447–450.

Harvey, J.R., Weeks, A.R., 1987. Recent development in a neutron dosimetry system based on the chemical etch of CR-39. Radiat. Prot. Dosim. 20, 89–93.

Meyer, P., Groetz, J.E., Fromm, M., Lacourt, A., Chambaudet, A., 1997. Neutron dosimetry at low and high fluences with CR-39. Radiat. Meas. 28, 423–428.

Nikezic, D., Yu, K.N., 2004. Formation and growth of tracks in nuclear track materials. Mater. Sci. Eng. R 46, 51–123.

Nikezic, D., Ng, F.M.F., Yip, C.W.Y., Yu, K.N., 2005. Application of the ray tracing method in studying α tracks in SSNTDs. Radiat. Meas. 40, 375–379.

Nikezic, D., Yu, K.N., 2008. Computer program TRACK_VISION for simulating optical appearance of etched tracks in CR-39 nuclear track detectors. Comput. Phys. Commun., in press, doi:10.1016/j.cpc.2007.11.011.

Popov, P.C., Pressyanov, D.S., 1997. Track density assessment by obstructed total internal reflection of a laser beam. Radiat. Meas. 27, 27–30.

Yu, K.N., Nikezic, D., Ng, F.M.F., Leung, J.K.C., 2005. Long-term measurements of radon progeny concentrations with solid-state nuclear track detectors. Radiat. Meas. 40, 560–568.

Yu, K.N., Lee, H.H.W., Wong, A.W.T., Law, Y.L., Cheung, S.F.L., Nikezic, D., Ng, F.M.F., 2007. Optical appearance of alpha particle tracks in CR-39 SSNTD. Nucl. Instrum. Meth. B 263, 271–278.